



Color removal from wastewater using a synthetic high-performance antifouling GO-CPTMS@Pd-TKHPP/polyether sulfone nanofiltration membrane

Foad Gholami¹ · Sirius Zinadini¹ · Soheila Nakhjiri Kamrani² · Ali Akbar Zinatizadeh^{1,3} · Kiumars Bahrami^{2,4}

Received: 31 May 2021 / Accepted: 17 September 2021 / Published online: 5 November 2021

© The Author(s), under exclusive licence to Springer-Verlag GmbH Germany, part of Springer Nature 2021

Abstract

Modified graphene oxide with 5,10,15,20-tetrakis-(4-hexyloxyphenyl)-porphyrin and palladium (II) (signified by GO-CPTMS@Pd-TKHPP) prepared as a novel antifouling polyether sulfone (PES) blended nanofiller membrane. The membrane efficiency has been analyzed such as pure water flux (PWF), hydrophilicity, and antifouling features. By increasing of modified graphene oxide percentage from 0 to 0.1 wt.% in the polymer matrix, the PWF was incremented from 14.35 to 37.33 kg/m²·h at 4 bar. The membrane flux recovery ratio (FRR) has been investigated by applying powdered milk solution; the FRR results indicated that the 0.1 wt.%-modified graphene oxide membrane showed a positive effect on fouling behavior with Rir and FRR value 8.24% and 91.76%, respectively. The nanofiltration membrane performance was assessed applying the Direct Red 16 dye rejection. It was demonstrated that the optimal membranes (0.1 wt.%-modified graphene oxide) had notable dye removal (99.58% rejection). The results are also verified by measuring the scanning electron microscopy (SEM), water contact angle (WCA), and atomic microscopy analysis (AFM).

Keywords Polyether sulfone · Nanofiltration membrane · Antifouling property · Modified graphene oxide · Dye removal · Wastewater treatment

Introduction

The most important environmental issue with colored wastewater is the removal of colors from the sewage (Elimelech & Phillip 2011). Industrial colored wastewater produced from textiles, paper, plastics, leather, food, and cosmetics must be

treated before wastewater drains into the environment (to recover paint) to prevent health hazards, and degradation of the ecosystem is separated and decomposed (Deka et al. 2014, Moradi et al. 2020). Membrane filtration as a very competitive candidate for water treatment technology has been considered for decades due to less energy efficiency, low cost-effectiveness, and stability compared to biological methods (Asadi et al. 2016, Gholami et al. 2020), adsorption (Balea et al. 2017, Balea et al. 2019), and photocatalytic degradation (Zangeneh et al. 2018, Zangeneh et al. 2019c). Because of this necessity, the application of the membrane processes among the modern methods for separation is of high interest for scientists (Ang et al. 2015, You et al. 2012). Polymeric membranes are very popular with regard to their excellent formation and their unique physicochemical properties in water refinery (Warsinger et al. 2018). The high flux permeation, acceptable solid elimination, and low clogging are integral requirements for the high efficiency of membrane filtration. Despite the hydrophobic nature of polymers, it leads to precipitation of foulant materials (pathogens, NOMs, proteins, polysaccharides, micropollutants, and color) on the surface

Responsible Editor: Angeles Blanco

✉ Sirius Zinadini
sirius.zeinadini@gmail.com

- ¹ Environmental Research Center (ERC), Department of Applied Chemistry, Faculty of Chemistry, Razi University, Kermanshah 67149-67346, Iran
- ² Department of Organic Chemistry, Faculty of Chemistry, Razi University, Kermanshah 67149-67346, Iran
- ³ Department of Environmental Sciences, University of South Africa, Pretoria, South Africa
- ⁴ Nanoscience and Nanotechnology Research Center (NNRC), Razi University, Kermanshah 67149-67346, Iran

of the membrane, which subsequently diminishes flux permeation (Hairom et al. 2014, Manda et al. 2014). The membrane's chemistry and morphology are affected by organic deposits that have destructive effects and are also an important barrier to the further development of membrane applications. Due to extensive research and efforts, one of the accepted solutions for membrane resistance to clogging for water treatment is to change and improve the membrane's hydrophilicity. The very good dispersion of nanofiller material in the entire membrane matrix, that so-called mix matrix membrane (MMM), in recent years, has brought a new concept for membrane fabrication with high flux, high rejection, and high fouling resistance (Mukherjee et al. 2019). Organic and inorganic nanoparticles due to having specific functional points such as high hydrophilicity, high specific surface area, and good correction can be used as appropriate filler to make nanocomposite membranes. The excerpted of nanomaterials that used in this field are metal–organic framework (MOF)(Emam et al. 2019), polycitrate alumoxane (PC-A)(Pirsaheb et al. 2019), SiO₂ nanoparticles (Ding et al. 2019, Zangeneh et al. 2019a), ZnO nanoparticle (Modi & Bellare 2019), zeolite (Mahmodi et al. 2020a, Mahmodi et al. 2020b), graphene oxide (GO)(Januário et al. 2020, Song et al. 2020, Yuan et al. 2020), and graphitic carbon nitride (g-C₃N₄) (Li et al. 2019).

Graphene oxide-based membranes (GO), which are made from two dimensions of GO nanostructures and polymer, are considered as promising candidates for water purification and desalination beyond traditional porous polymer membranes

(Fathizadeh et al. 2017, Hegab & Zou 2015). Considering the high adaptability, high mechanical strength, high surface hydrophilic nature, and 2-D interrelation structure for the separation of ions as well as displacement of molecules, graphene oxide-based membranes have exhibited excellent performance in relation to high flux and impressive antifouling (Huang et al. 2013, Koltonow & Huang 2016, Papageorgiou et al. 2015). Because of agglomeration and the electrostatic repulsion between nanosheets graphene oxide in aqueous solutions, the water stability of the unpolished graphene oxide is weak and tends to break down normally. Therefore, researchers have provided many modifications to solve this problem (Chen & Yan 2010, Hua et al. 2015, Wang et al. 2011).

Today, researchers have shown that the hydrophilicity of graphene oxide with hydrophilic agents helps to solve the problem of decomposition and clogging of GO and GO-based membranes, which strongly suggest that this strategy will help to reduce the contamination of pollutant by modified membranes (Cote et al. 2010, Hu et al. 2016, Lee et al. 2004). In cases of reducing the membrane fouling and degradation of nanosheets by combining triethanolamine (TEOA) with modified titanate nanowires (TNWs) and graphene oxide, Liu and his colleagues have made photocatalytic membranes that were able to solve membranes and graphene oxide problems. The results (flux: 42 L/m²·h; dye rejection: 95%) show that the modified membrane, due to its efficient modifications, has a high degree of antifouling and hydrophilicity that was used to

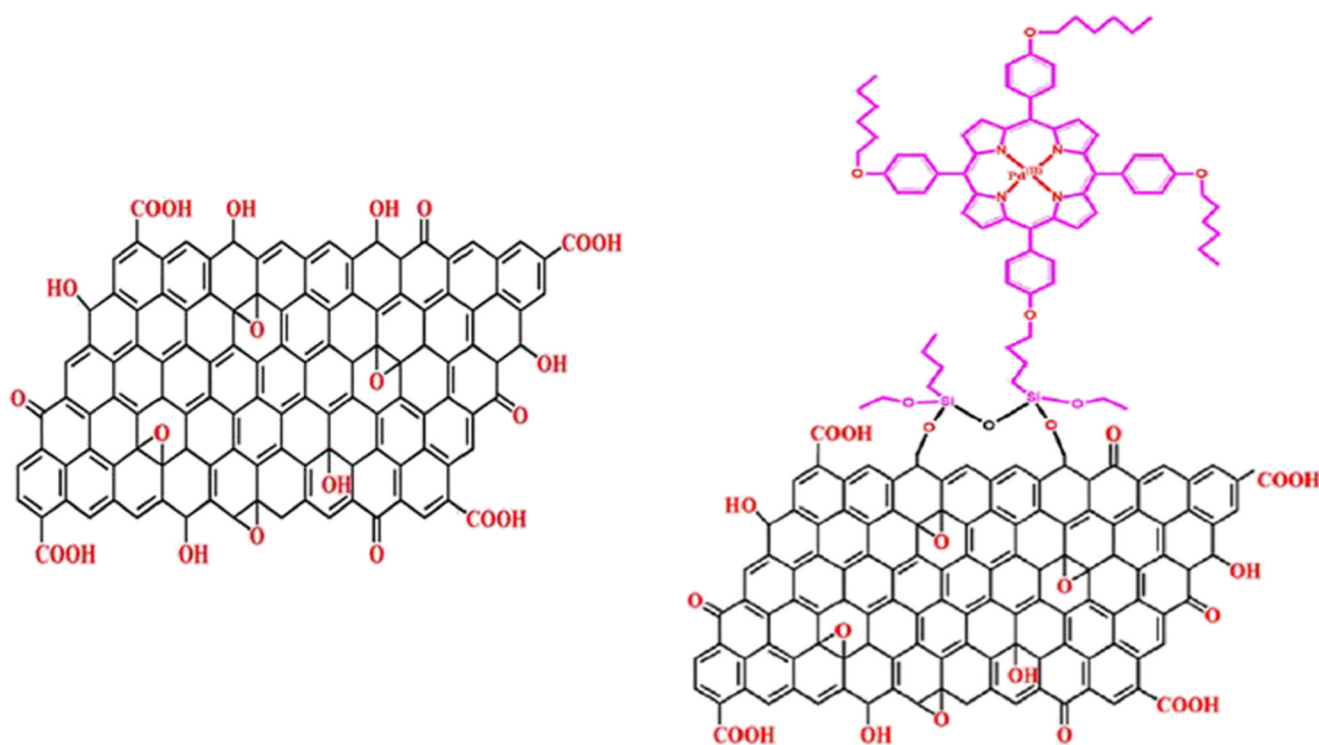


Fig. 1 Scheme of GO and GO-CPTMS@Pd-TKHPP

Table 1 Casting solution compositions

Membrane type	PES (wt.%)	PVP (wt.%)	Modified graphene oxide (wt.%)	DMAc (wt.%)
M ₁	20.0	1.0	0.0	79.0
M ₂	20.0	1.0	0.1	78.9
M ₃	20.0	1.0	0.5	78.5
M ₄	20.0	1.0	1.0	78.0

remove Congo Red dye (Liu et al. 2017b). Huang et al., in 2014, developed a combination of graphene oxide and metal-organic framework (ZIF-8) to improve the membrane’s performance for better separation of gasses, which in bicontinuous ZIF-8@GO-based membrane increased hydrogen permselectivity relative to the unmodified state due to the presence of graphene oxide (Huang et al. 2014). In the next work that was introduced in 2017, Ayyaru and Ahn donated hydrophilicity and antifouling properties to the PVDF nanocomposite ultrafiltration membranes by inserting sulfonated graphene oxide (SGO). According to the results, due to the

improvement of the graphene oxide by the –SO₃H agent, the water permeation flux increased 146.6% and flux recovery ratio (88.7%) compared to the unmodified graphene oxide (water flux: 53.3%; FRR: 75%), indicating that the problem of graphene oxide and the membrane have also been resolved (Ayyaru & Ahn 2017). In 2018, Abdi and coworkers presented a hybrid combination (metformin/GO/Fe₃O₄) that was successfully introduced into the polymeric membrane for the removal of colored materials and heavy metals. The results of this combination were high hydrophilicity, PWF and antifouling effect, which has been applied to remove direct red-16 and

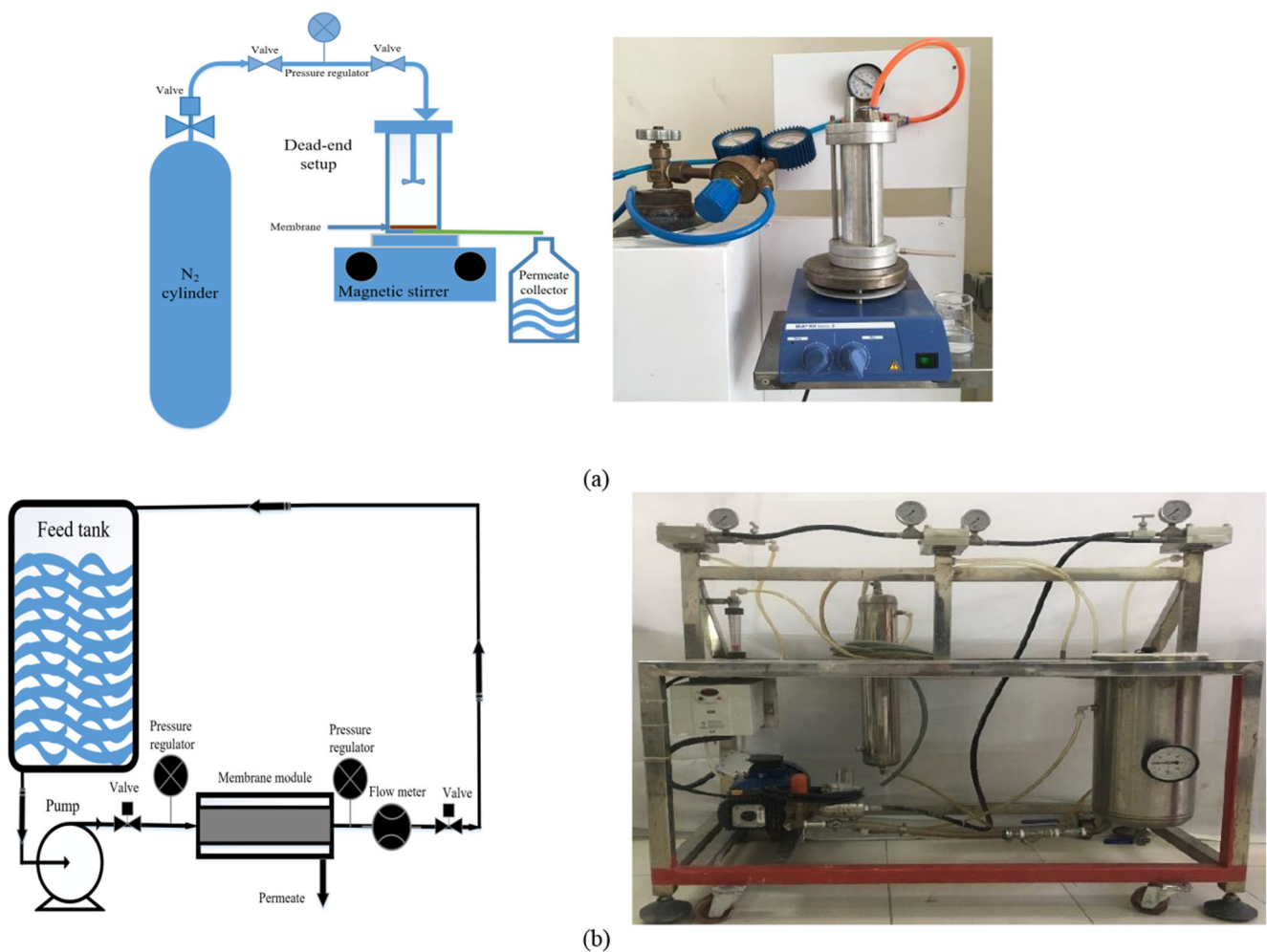


Fig. 2 Schematic of the (a) dead-end setup and (b) cross-flow setup

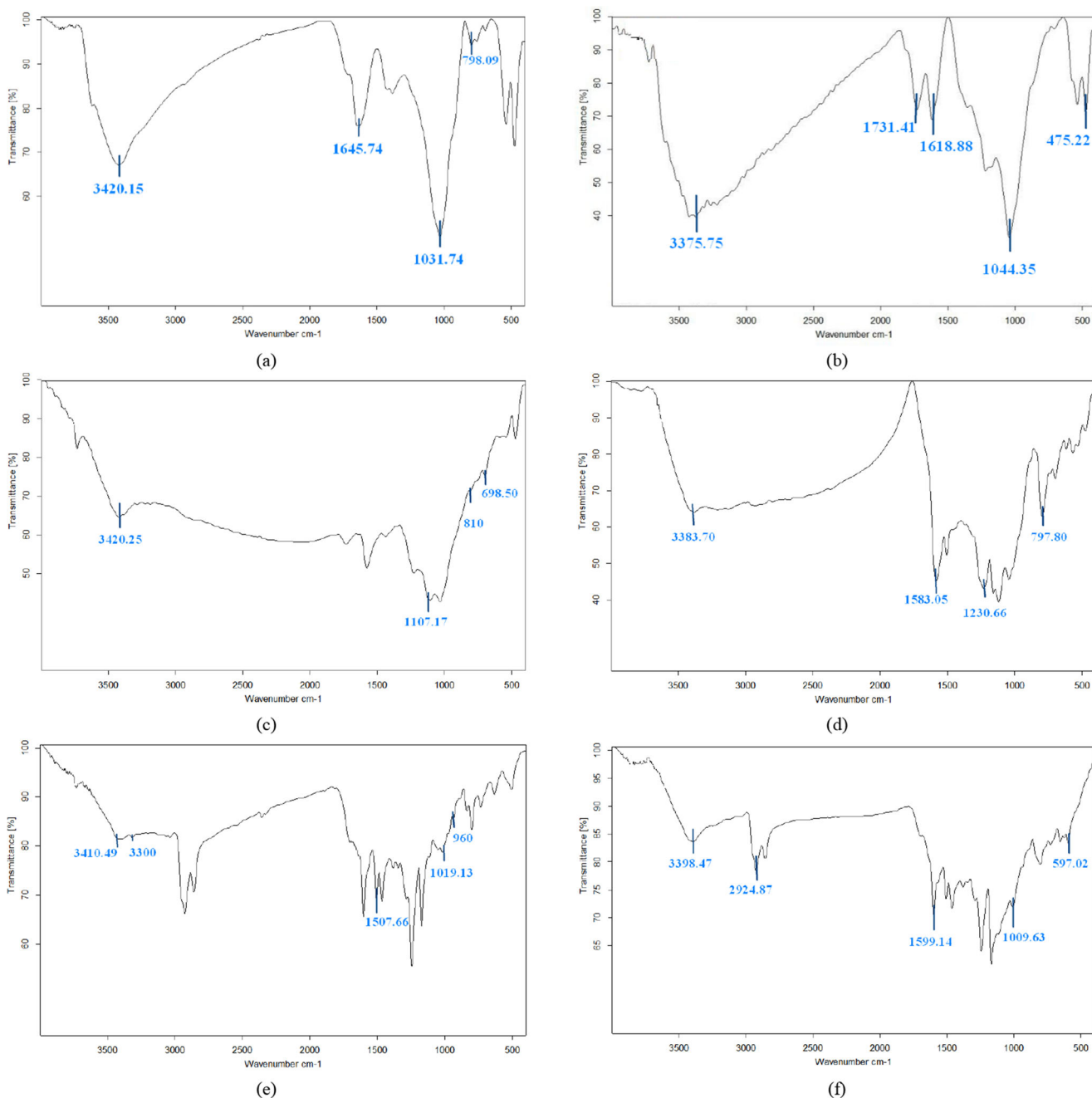


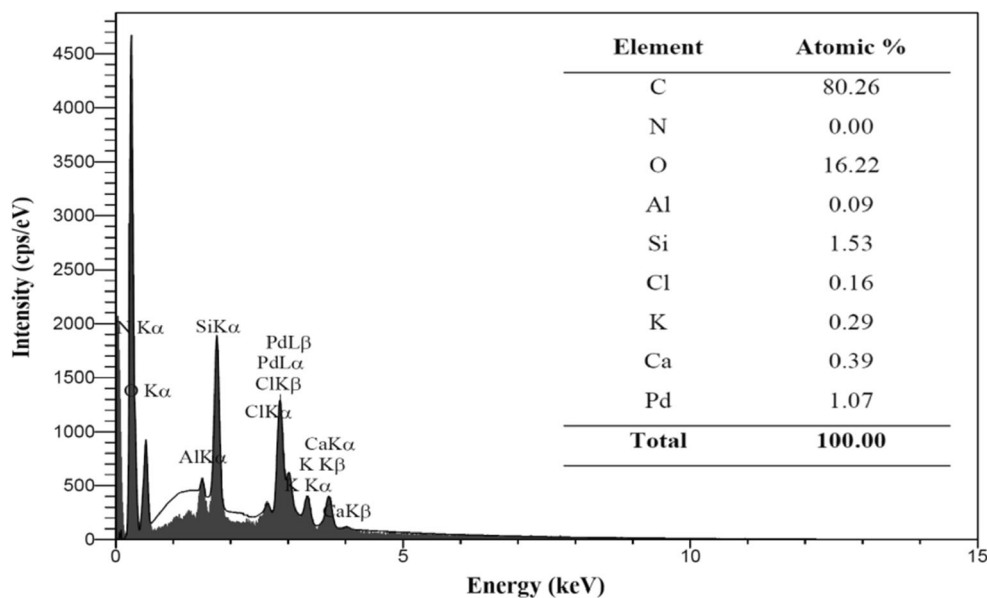
Fig. 3 FT-IR spectrum of (a) FT-IR spectra of GO, (b) GO-OH, (c) GO-CPTMS, (d) GO-CPTMS@THPP, (e) GO-CPTMS@TKHPP, and (f) recycled GO-CPTMS@Pd-TKHPP

copper ions with 99% and 92% removal, respectively (Abdi et al. 2018). The graphene oxide framework built by use of 1,4-cyclohexanediamine (CDA) and p-phenylenediamine(pPDA) was introduced by Qian and et al. in 2018 and exposed in the field of modified graphene oxide. The synthesized composition was used in the alumina membrane, which showed great results, that can be mentioned to high flux (20.1 kg/m²·h) and high ionic rejection (99.9%) (Qian et al. 2018).

According to our studies, no publication has been found on the use of GO modified by CPTMS@Pd-TKHPP to improve

nanofiltration membrane for colored effluent separation. In this study, with the aim of increasing membrane hydrophilicity and decreasing the water contact angle, the hydrophilic functional groups were added amine, aromatic rings –COOH, –OH, =O, and Pd metal. The addition of non-bounded lone pairs and double bonds as well as hydrophilic functional groups can create an aqueous layer on the surface of the membrane that helps to prevent the formation of a foulant layer on the membrane surface. It was also expected that the addition of aromatic rings during the nanoparticle

Fig. 4 GO-CPTMS@Pd-TKHPP EDX pattern



modification would increase membrane porosity which can improve the membrane pure water flux by itself. As a notice, this modification can be used to construct a novel membrane by the phase inversion method. In the current study, the membrane modified with GO-CPTMS@Pd-TKHPP was firstly synthesized and characterized. In order to identify membrane characteristics, water contact angle, SEM, AFM, and antifouling tests are used. It should be mentioned that the optimal membranes have been used to reject dye from wastewater.

bromohexane were prepared from Sigma Aldrich, USA. Graphite powder, 3-(chloropropyl)-trimethoxysilane palladium (II) chloride, dimethylformamide (DMF), and ethanol were prepared from Merck, Germany. All the chemical reagents used in our experiment were used without further purification.

Materials and methods

Materials

The polyvinyl pyrrolidone (PVP) ($M_w = 25,000$ g/mol) was obtained (Merck Co., Germany). Dimethylacetamide (DMAc) and PES ($M_w = 58,000$ g/mol) were pouched (BASF Co., Germany). In all experiments, distilled water has been used. 4-Hydroxy benzaldehyde and 1-

Modified graphene oxide nanocomposites preparation

The GO-CPTMS@Pd-TKHPP (Fig. 1) was synthesized by the following methods.

According to the usual way, graphene oxide (GO) was prepared based on modified hummers method from graphite powder (Zaaba et al. 2017); then graphene oxide-3-(chloropropyl)-trimethoxysilane (GO-CPTMS) was synthesized by adding CPTMS to GO in a solution of toluene; then the mixture was stirred and refluxed for 24 h at 110°C; the solid was filtered and dried; after this, 4, 5,10,15,20-tetrakis-(4-hydroxyphenyl)-porphyrin (THPP) was prepared; synthesis of THPP was achieved according to the following procedure. Pyrrole was leisurely added under stirring to a solution of 4-hydroxy benzaldehyde in refluxing propionic acid. Refluxing was continued for 2 h; after this step, the reaction mixture was washed several times and cooled slowly, filtered, and dried; the dark purple crystalline product was precipitated. Then, THPP was added to a solution of GO-CPTMS in refluxing dioxane, and in the presentation of Na_2CO_3 and KI, a black powder of GO-CPTMS@THPP was obtained. Next 3-(chloropropyl)-trimethoxysilan 5,10,15,20-tetrakis-(4-(hexyloxy) phenyl)-porphyrin GO-CPTMS@Pd-TKHPP was obtained by adding 1-bromohexane to a solution of DMF and K_2CO_3 (4:4) in a flask

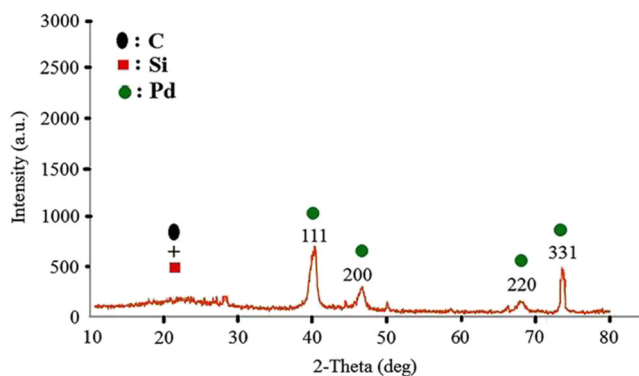


Fig. 5 GO-CPTMS@Pd-TKHPP XRD pattern

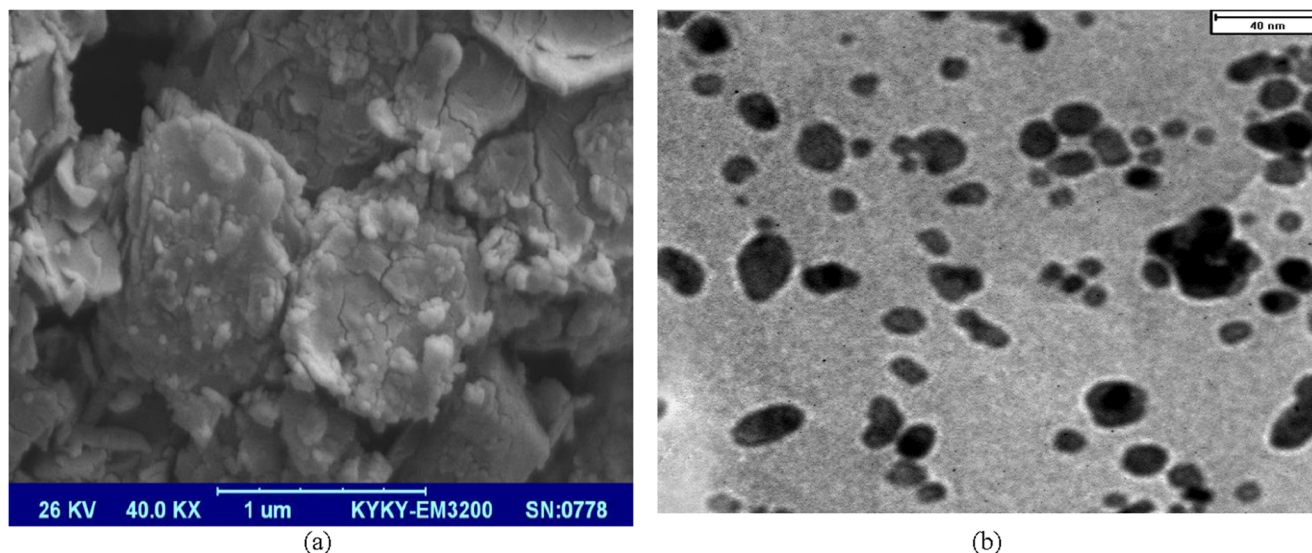


Fig. 6 (a) GO-CPTMS@Pd-TKHPP SEM images and (b) GO-CPTMS@Pd-TKHPP TEM images

and GO-CPTMS@THPP; then, the obtained mixture was refluxed up for 24 h, then dried, and the gray powder was obtained. Finally, GO-CPTMS@Pd-TKHPP was obtained by adding PdCl₂ to GO-CPTMS@Pd-TKHPP in the presence of ethanol solvent and reflux condition for nearly 24 h (Bahrami & Kamrani 2018).

Preparation of modified mixed matrix PES-GO membrane

The unmodified and modified membranes were carried out via the phase inversion method. The membrane solution composition for all cases has been listed in Table 1. In order to form the homogenous solution, first, a proper amount of modified GO was added into DMAc and sonicated (DT 102H Bandelin ultrasonic (Germany)) for 30 min. Then, PVP and PES were added to obtain the solution. After this step, the casting solution was kept on a continuous stirrer overnight at room temperature. Finally, in order to increase the amount of homogeneity, dope solutions were sonicated again (20 min) to make sure all air bubbles had been removed and impressive dispersing was done. Finally, by using a self-made knife, the solutions were casted on glassy plates (150- μ m thickness) and immediately (without evaporation) moved to distilled water (nonsolvent bath at RT). After forming the polymeric membrane, they were moved to fresh distilled water (24 h). This will remove water-soluble components from the membrane matrix. Finally, the obtained membranes were warped between paper for drying (24 h) (Zinadini et al. 2014).

Characterization of modified GO membranes

The membrane morphology was considered by applying a scanning electron microscope (SEM)(Philips-XL30, the

Netherlands) (20 kV acceleration voltage); first, membranes were cut and cleaned with filter paper to clean probable contaminants. Then, they were immersed into liquid nitrogen for 50–70 s. After that, for membrane drying, the frozen membranes were breaking and kept at RT (room temperature). Afterward, the dried membranes were coated by Au ion in order to produce electron conductivity. As the final step, SEM images were captured (20 kV in high vacuum condition).

The surface roughness for the prepared membrane was analyzed by applying atomic force microscopy (AFM) (Nanosurf® Mobile S (Switzerland)); this device was equipped with an optical probe microscope. Small square samples were prepared (2*2 cm) and fixed on a holder, and the surface was scanned (4.4 μ m *4.4 μ m). The results reflected as (Sa) mean roughness, the root of square data (Sq), and the average difference between the highest peak and the lowest valley (Sz) has been achieved with quantitative analysis.

A recent method to analyze the hydrophilicity of membranes is water contact angle (WCA) (G10, KRUSS, Germany) measurement. The propensity of small distilled water droplets to extend on the membrane surface is known as membrane hydrophilicity. For WCA measurement, in all cases, 2 μ l of deionized water has been used. For reducing experimental errors, all examinations were repeated in 4 random sites and the mean value was reported.

Membrane performance

Pure water flux and antifouling experiments

Membrane performance, pure water flux (PWF), and antifouling attributes of modified NF membranes with GO were

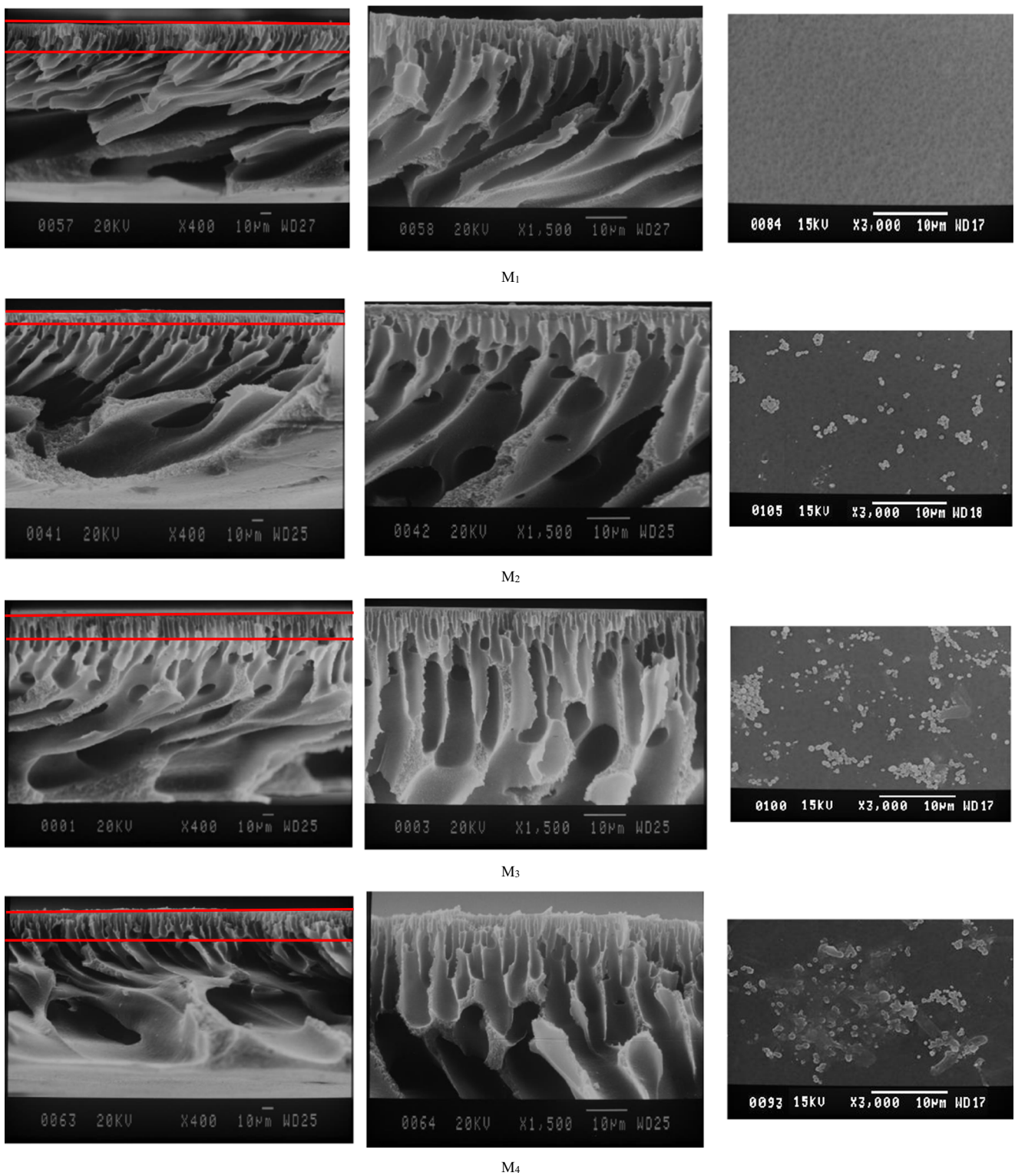
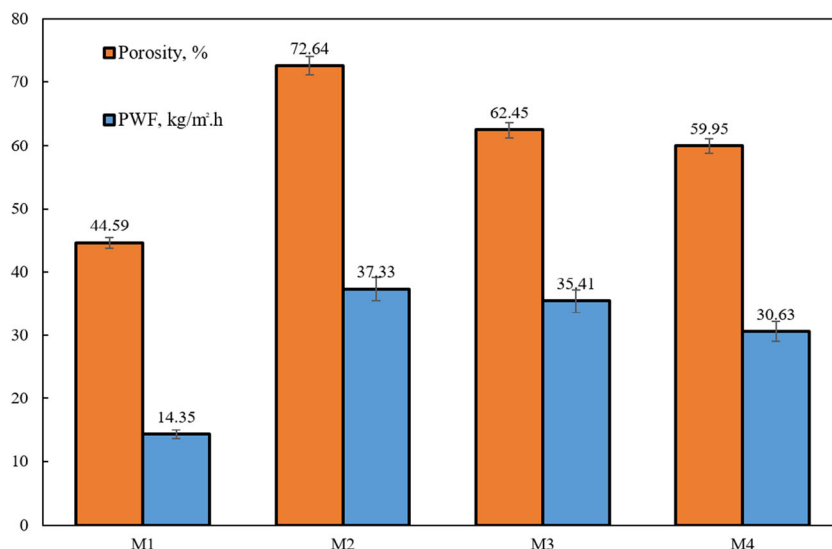


Fig. 7 SEM images cross-section and surface (M₁ =unfilled.%, M₂ = 0.1 wt.%, M₃ = 0.5 wt.%, and M₄ = 1.0 wt.%)

examined in a dead-end setup (Fig. 2a) (150 ml and 12.56 cm²). As trans membrane pressure (TMP) nitrogen cylinder, the cell was equipped to force the feed pass through the membrane. In order to concentrate polarization reduction, constant simulation

was applied for the cell (400 rpm). In order to earn a stable state, for the first 30 min of the experiment, the TMP was compressed at 5 bar and then it was reduced to 4 bar (Gholami et al. 2017). Based on Eq. (1), the PWF was calculated as

Fig. 8 PWF and porosity of the modified graphene oxide blended PES nanofiltration membranes (M_1 = unfilled, M_2 = 0.1 wt.%, M_3 = 0.5 wt.%, and M_4 = 1.0 wt.%)



$$J_{W,1} = \frac{M}{A\Delta t} \quad (1)$$

where Δt is the time of permeation, A (m²) is touching surface, and M is the weight of permeation.

Milk powder solution (8000 ppm), to consider the antifouling properties were tested as proper foulant (after PWF test). The milk powder permeation (J_P (kg/m².h)) was tested based on water permeation during the analysis (4 bar, 90 min). After that test, the fouled membrane was cleaned with deionized water (15 min immersed in water without any backwash), then the pure water flux was tested again with distilled water. Based on the following equation, the FRR can be calculated as

$$FRR = \left(\frac{J_{W2}}{J_{W1}} \right) \times 100 \quad (2)$$

As a matter of fact, higher FRR for membranes indicates the distinct antifouling ability of the nanofiltration membranes.

Following the results in order to consider antifouling behavior, during filtration resistance fouling ratio was evaluated in detail, irreversible fouling (R_{ir}), reversible fouling (R_r), and total fouling (R_t) were investigated according to the following equations:

$$R_t(\%) = \left(1 - \frac{j_p}{j_{w1}} \right) \times 100 = R_{ir} - R_r \quad (3)$$

$$R_r(\%) = \left(\frac{j_{w2} - j_p}{j_{w1}} \right) \times 100 \quad (4)$$

$$R_{ir}(\%) = \left(\frac{j_{w1} - j_{w2}}{j_{w1}} \right) \times 100 \quad (5)$$

Dye removal

As dye-containing azo groups, direct red-16 was chosen. In this case, to consider membrane efficiency, the filtration was operated in a dead-end setup (120 min at 4 bar); each run was tested by 150 ml of feed. After this step, in order to evaluate long-term filtration and industrial simulation, a cross-flow setup (Fig. 2b) was applied (driving force 4 bar, flow rate 300 L/h at 420 min). In all experiments to propose feed simulation, 50 mg/L of direct red-16 was chosen, which is in the range of typical textile wastewater industries. As a result, the flux recovery ratio and flux were reported based on Eqs. (1) and (2). By using UV-Vis spectrophotometer (520 nm for direct red-16 and 665 nm for methylene blue) (JENWAY 6320D), according to Eq. (6), the rejection was calculated as

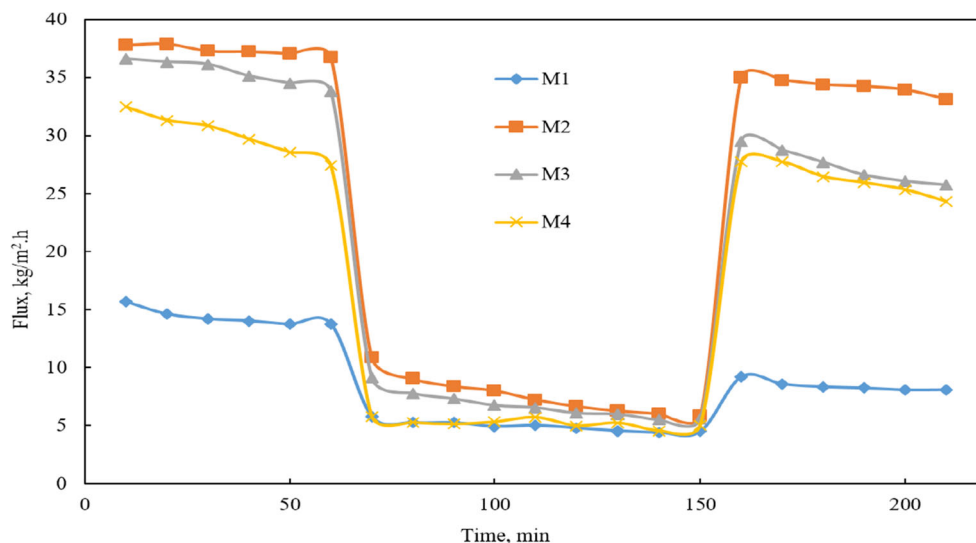
$$(\%) = \left(1 - \frac{C_p}{C_f} \right) \times 100 \quad (6)$$

where C_f is feed concentration and C_p is permeated concentration of dye (mg/L).

Table 2 Water contact angle and pore size of the produced nanofiltration MMM

	M_1	M_2	M_3	M_4
Water contact angle, °	75.22 ± 1.50	59.20 ± 1.18	54.70 ± 1.09	50.20 ± 1.00
Pore size, nm	3.0	1.6	2.1	2.6

Fig. 9 Flux against the time of the membranes with different concentrations of modified graphene oxide nanosheets. The filtration process includes three phases (water flux, milk powder filtration, and second water flux) after washing fouled membranes (M_1 = unfilled, M_2 = 0.1 wt.%, M_3 = 0.5 wt.%, and M_4 = 1.0 wt.%)



Results and discussion

Modified graphene oxide nanocomposites characterization

The prosperous synthesis of the GO-CPTMS is confirmed by the FT-IR spectra (Fig. 3c). The peak turning up at 810 cm^{-1} comes back to Si–O–Si, the symmetric vibration. The peak at 1107 cm^{-1} is relevant to asymmetrical Si–O–Si stretching. About GO-CPTMS@TKHPP (Fig. 3e), it recognized that the peak of the N–H bending and stretching frequencies are located at $\sim 3300\text{ cm}^{-1}$ and $\sim 960\text{ cm}^{-1}$ and shown free base porphyrins. When the PdCl_2 was interred into the porphyrin ring, the N–H peak vibration of free base porphyrins vanished and features of the functional groups of Pd–N bond shaped at $\sim 1009\text{ cm}^{-1}$ (Fig. 3f), that analyzed the configuration of a metal–ligand bond (Bahrami & Kamrani 2018).

In Fig. 4, the EDX analysis of nanosheets (GO-CPTMS@Pd-TKHPP) displayed the attendance of the anticipation elements in the nanosheets of GO, such as silicon, oxygen, palladium, nitrogen, and carbon. As can be seen, the element distribution of the Si-Pd/GO is approximately 1.43 (Zhang et al. 2017).

XRD pattern of GO-CPTMS@Pd-TKHPP as nanostructure exhibits peaks at $2\theta = 40.4, 46.8, 68$ and 74.1° which correspond to (111), (200), (220), and (331) crystalline planes of Pd, respectively, illustrated that Pd element does not exist in

the form of Pd(II) and it was shown Pd (0)(Fig. 5) (Fareghi-Alamdari et al. 2016, Zolfigol et al. 2013).

The stratification structure of GO-CPTMS@Pd-TKHPP was also perceived from transmission electron microscopy (TEM) and scanning electron microscopy (SEM). The scanning electron microscopy (SEM) illustration of GO-CPTMS@Pd-TKHPP (Fig. 6a) shows the ingredient scale, morphology, and superficies sameness. Transmission electron microscopy (TEM) image of the GO-CPTMS@Pd-TKHPP indicated which Pd(II)-TKHPP was seated on the surface of graphene oxide (Fig. 6b)(Bahrami & Kamrani 2018).

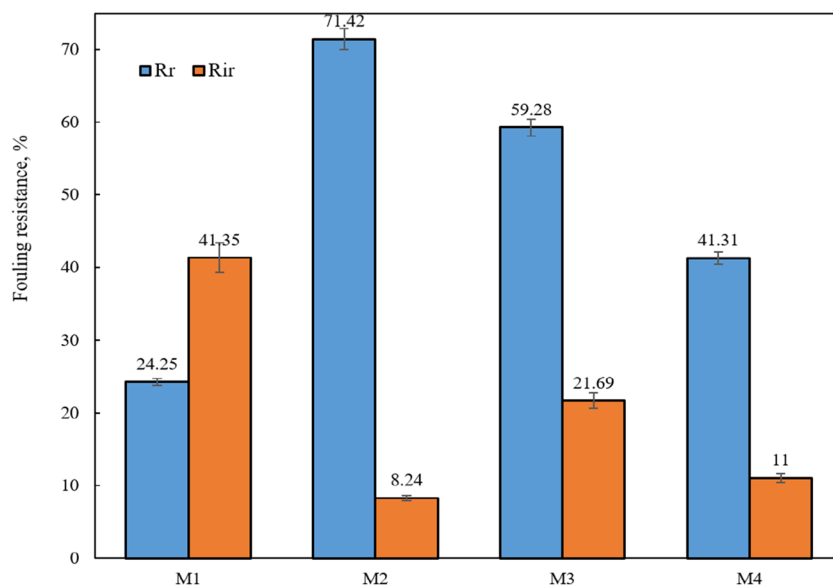
Morphology analysis

In order to consider the effect of GO-CPTMS@Pd-TKHPP, concentration on the structure and morphology of the membrane and SEM images are shown in Fig. 7. As shown in the picture, asymmetric structure with a uniform dispersion of nanoparticles is visible and can be easily recognized as finger-like pores with the thin top layer and thick bottom layer due to fast immigration of hydrophilic NPs in the phase inversion step. The identical building of the membranes implies that the impact of nanoparticles on morphology was low. So, this result shows that it was not an important influence on the formation of mold membrane. Small differences in the structure of membranes at low concentrations were observed that described the increase in porosity and consequently increased the radius of pores. In different concentrations of nanoparticles, 0.1 wt.% provided the minimum thickness of the top layer in the membrane. As seen in Fig. 8, by adding 0.1 wt.% modified graphene oxide nanocompound, the porosity was increased, and a further increase in the amounts of the nanosheets to more than 0.1 wt.% caused the reduction of pore radius (Vatanpour et al. 2011).

Table 3 FRR of the prepared nanocomposite membranes infiltration of powdered milk solution

	M_1	M_2	M_3	M_4
Flux recovery ratio, %	58.65	91.76	78.3	88.99

Fig. 10 Fouling resistance ratio of modified graphene oxide-PES ultrafiltration membranes (M_1 = unfilled, M_2 = 0.1 wt.%, M_3 = 0.5 wt.%, and M_4 = 1.0 wt.%)



The prepared membranes pure water flux and hydrophilicity

Water contact angle measurement can be used to identify the hydrophilicity surface of prepared membranes. As illustrated in Table 2, by adding nanofiller to the membrane matrix, a logical trend on WCA reduction can be observed. It should be noted that, due to presenting a hydrophilic functional group on the GO, the membrane hydrophilicity was increased (membrane contact angle was decreased), causing an increase in membrane permeability due to hydrogen bonding between water and membrane surface.

Flux transmission depends on many factors, that hydrophilicity is one of the most important cases. The hydrophilic functional groups of the GO-CPTMS@Pd-TKHPP on the membrane surface caused a change in the pure water flux (PWF) that established hydrogen bonds between water molecules and membrane surface (Table 2). Adding the nanoparticles up to 0.1 wt.% led to an increase in PWF (M_2). By adding nanoparticles to the membrane matrix, an increment is notable for M_2 . In higher loadings (M_3 , M_4), the accumulation effect that caused PWF reduction might be due to porosity occupation (Fig. 8). It should be noted that the powdered milk

solution rejection was more than 98%, showing the interrelation between flux increment and defects or cracks in the membrane due to a poor bond between the modified graphene oxide and PES.

Fouling behavior of the prepared membranes

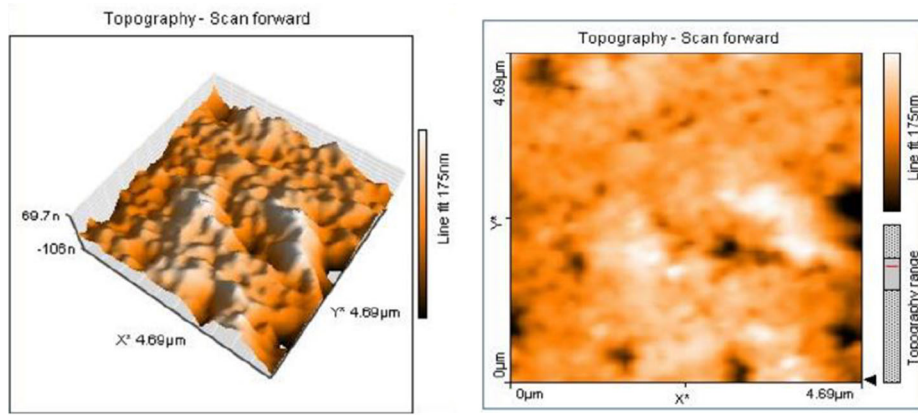
Figure 9 shows the antifouling performance of the prepared membrane in three-step filtration. The results of 0.1 wt.% of modified graphene oxide (M_2) demonstrated the highest permeability compared to the other concentrations. As can be obtained (Fig. 9), the difference in flux, in the first step and third step, observed between the modified and unmodified membranes is caused by the presence of hydrophilic function group on the GO surface, which has been donated to have a hydrophilic effect on the PES membrane.

FRR is one of the important parameters for antifouling assessment. The FRR diagram was displayed in Table 3. The greatest FRR for membrane has been achieved for membrane embedded with 0.1 wt.% (M_1) of modified graphene oxide. Antifouling performance of embedded mixed matrix membranes could be related to hydrophilicity for modified membranes, although this effect has an optimal ratio (M_2) in higher additives due to agglomeration effect on the acceptable trend (FRR reduction) is notable. That was induced by remaining functional groups of GO-CPTMS@Pd-TKHPP on the membrane surface. Creating a hydration layer on the membrane surface due to the presence of hydrophilic nanosheets and hydrogen bonding can inhibit the formation of a foulant

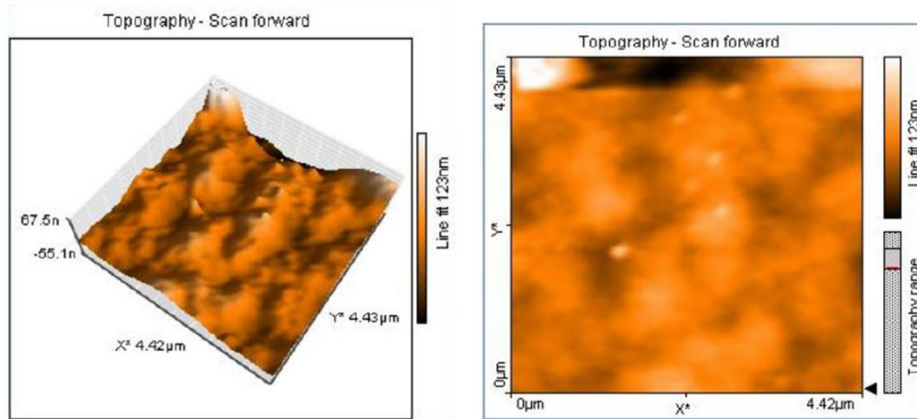
Table 4 Membrane surface roughness of modified graphene oxide filled nanofiltration PES membranes

Membrane	S_a (nm)	S_q (nm)	S_z (nm)
M_1	21.251	28.671	245.15
M_2	8.003	10.014	67.483
M_3	8.755	11.363	103.83
M_4	9.707	14.705	162.8

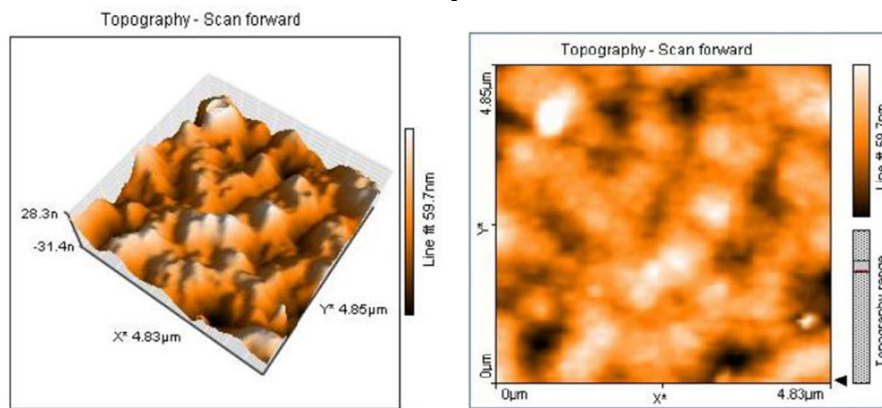
Fig. 11 3D and 2D AFM images of the modified graphene oxide nanofiltration PES membranes (M_1 = unfilled, M_2 = 0.1 wt.%, M_3 = 0.5 wt.%, and M_4 = 1.0 wt.%)



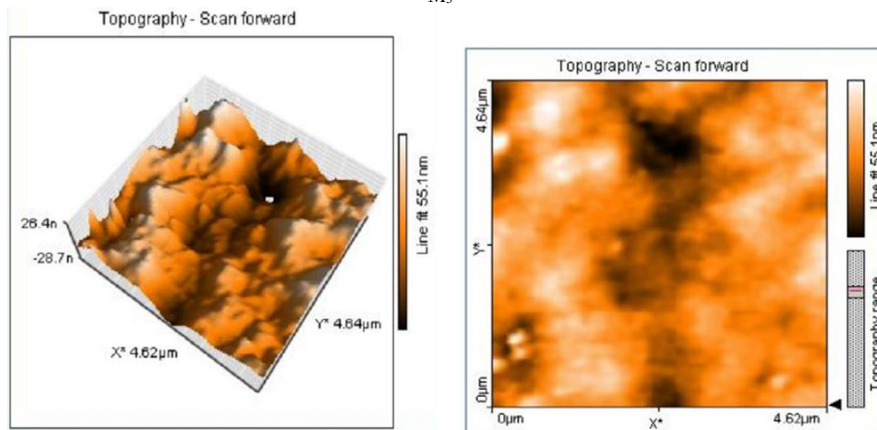
M₁



M₂



M₃



M₄

layer on the membrane surface. The results demonstrated that the addition of the modified graphene oxide nanosheets (ingenious design with effective groups) in the PES membrane was useful to improve membrane permeability (Ng et al. 2013).

According to the deposition phenomenon, resistance parameters as irreversible fouling resistance (R_{ir}) and reversible fouling resistance (R_r) were obtained, as shown in Fig. 10. Irreversible fouling resistance of membrane embedded with 0.1 wt.% nanoparticles has reached the lowest value, but R_r has also increased with increasing concentration. The trapped residual foulants into the membrane pores and valley surface are responsible for irreversible aggregation, which noticeably can be removed by the washing process (immersing in water). The M_2 membrane (embedded with 0.1 wt.% modified graphene oxide) indicated the highest FRR (91.76%).

AFM technique was used for measuring the membranes' surface roughness. As a matter of fact, lower roughness replies to stronger antifouling property. In addition, foulants may be trapped in the valleys of the membrane with unusual surfaces, resulting in clogging of the valleys. The AFM and its associated results are presented in Fig. 11 and Table 4. The average roughness (S_a) of the bare nanofiltration membrane changed from 21.251 to 8.003 nm for the modified membranes with 0.1 wt.% of GO-CPTMS@Pd-TKHPP and then enhanced to 9.707 nm for the modified graphene oxide 1 wt.%. In the lower concentration of modified graphene oxide, because of less electrostatic interactions between the modified graphene oxide, they are tidied in membrane symmetrically, resulting in a smooth membrane surface. But due to the increment in agglomeration and pore size of modified graphene oxide, membrane surface roughness was enhanced at a higher concentration of modified graphene oxide (Zangeneh et al. 2019a).

Dye removal efficiency

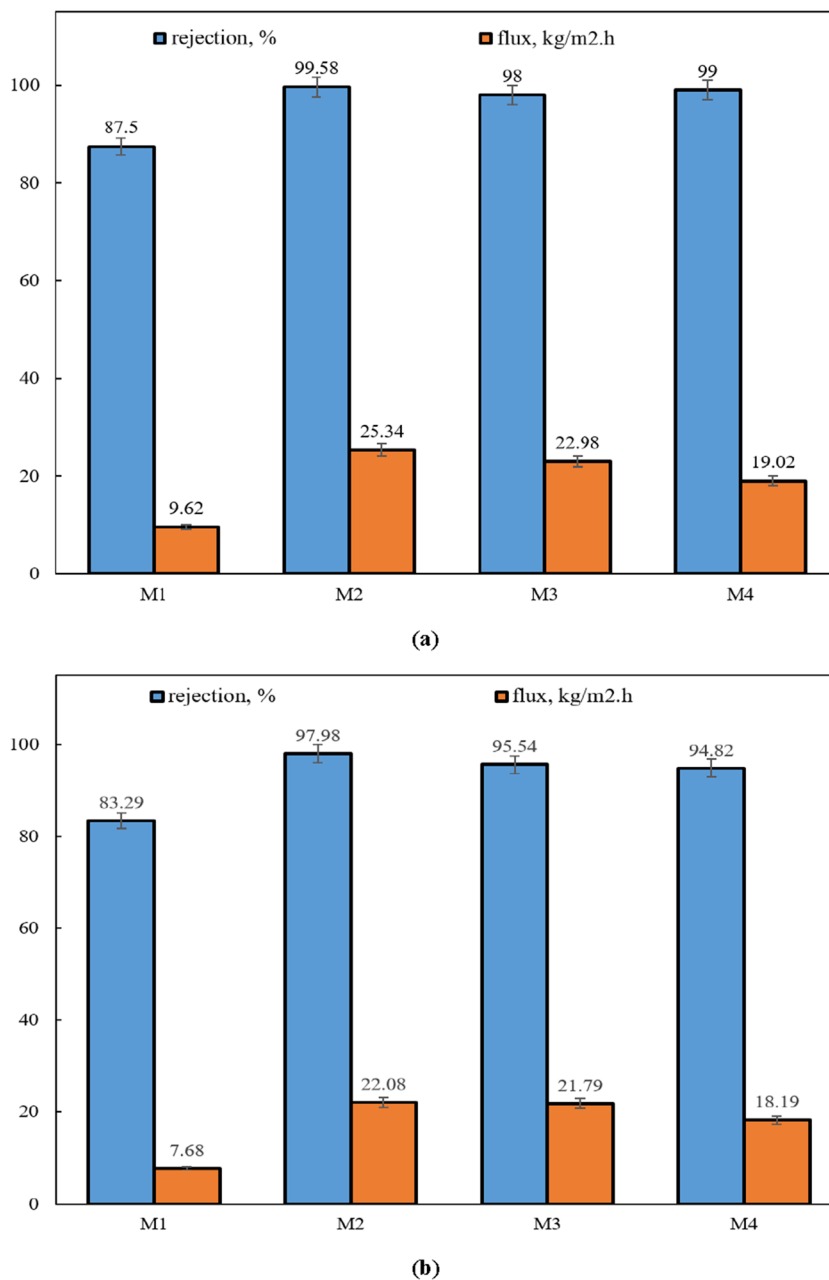
Rejection and performance

The dye rejection results are indicated in Fig. 12, that described the membrane capability for direct red 16 and methylene blue dye removal from simulated feed (50 mg/L) after 60-min filtration as a function of the modified graphene oxide percentage in the casting solution. The dye removal efficiency for the modified membrane (M_2) was achieved at 99.58% and 97.98% for direct red 16 and methylene blue, respectively. Although the removal percentage for M_1 is lower (87.5% and 83.29%, respectively). This is caused by the presence of hydrophilic nanofiller in the membrane structures (Table 2) as an excellent refining agent (Wang et al. 2011). This high removal percentage of colored materials can be attributed to two factors: (i) chemical interactions (non-covalent bonds and π - π stacking) and (ii) electrostatic repulsion between color and membrane surface. In other words, because the direct red 16 and surface of the membrane both have a negative charge, they repel each other (given the existence dispersion of negative groups at the matrix of the dye molecule, the direct red-16 indicates a negative nature at the neutral pH), as well as non-covalent bonds (hydrogen bond) and π - π stacking between the agents of direct red 16 ($-\text{SO}_3$, $-\text{NH}_2$, $-\text{OH}$, and aromatic rings) and distributed GO-CPTMS@Pd-TKHPP on the membrane surface, prevent passing of dye through the membrane and for these reasons that the removal efficiency was more than 99% (Sabbatini et al. 2010, Zhang et al. 2019, Zhou et al. 2019). Although, as shown in Fig. 12 for methylene blue (aromatic rings $-\text{N}$ and $-\text{S}$), the removal percentage has decreased which caused the positive nature of the methylene blue and low molecular weight in methylene blue than direct red 16 (methylene blue and direct red 16 molecular weight: 319.85 g/mol and 637.55 g/mol, respectively), so it is possible

Table 5 Comparison of dye separation performance of synthesized membranes with other works in literature

Membrane types	Dye types	Molecular weight, g/mol	Dye concentration, mg/l	Dye rejection, %	Dye flux, kg/m ² ·h	Ref
PSF/PEG/ZnCl ₂	Congo red	696.65	200	98	10	Panda and De 2014)
	Crystal violet	407.98		98	8	
	Chrysoidine R	262.74		95	10	
PES/GO/TiO ₂	Reactive green 19	1418.93	100	99	-	Safarpour et al. 2016
	Reactive blue 21	377.43		81.4	-	
	Direct yellow 12	1680.66		95.4	-	
PES/ HNTs-SO ₃ H	Reactive black 5	991.82	1000	90	-	Wang et al. 2015
	Reactive red 49	576.49		80-90	-	
PES/CS/MMT	Reactive black 5	991.82	500	96	40	Zhu et al. 2015
	Reactive red 49	576.49		93	40	
PES/Cellulose	Direct red 23	813.73	1000	98	-	Lessan et al. 2016
	Direct red 79	1048.87		95	-	
PES/GO-CPTMS@Pd-TKHPP	Direct red 19	637.55	50	99.58	25.34	This work
	Methylene blue	319.85		97.98	22.08	

Fig. 12 Dye separation efficiency of modified graphene oxide-PES membranes, (a) direct red 16 and (b) methylene blue



methylene blue to pass through the membrane and results show the dye removal reduction for methylene blue than direct red 16 (Fig. 12). It should be noted that the permeation flux of dye solutions was slightly lower than the pure water flux due to the adsorption of dye molecules on the membrane surface

and the concentration polarization. According to the initial concentrations of direct red 16 (50 mg/L), the excellent rejection was obtained 99.58%, but for precise evaluation of the dye rejection at a high concentration (200 mg/L), the dye rejection was also investigated that achieved 97.29% (Bouazizi et al. 2017, Liu et al. 2017a); also, in Table 6 comparison, the performance of dye removal is provided (Table 5).

Table.6 Long-term results for dye rejection

Membrane	Flux, kg/m ² .h	FRR, %	Direct red-16 rejection, %
M ₁	15.29	68.42	89.61
M ₂	54.44	97.67	99.98

Long-term behavior

The results of long-term performance during the treatment of colored wastewater by the cross-flow system are displayed in

Fig. 13 Long-term filtration for dye removal (M_1 = unfilled, M_2 = 0.1 wt.%)

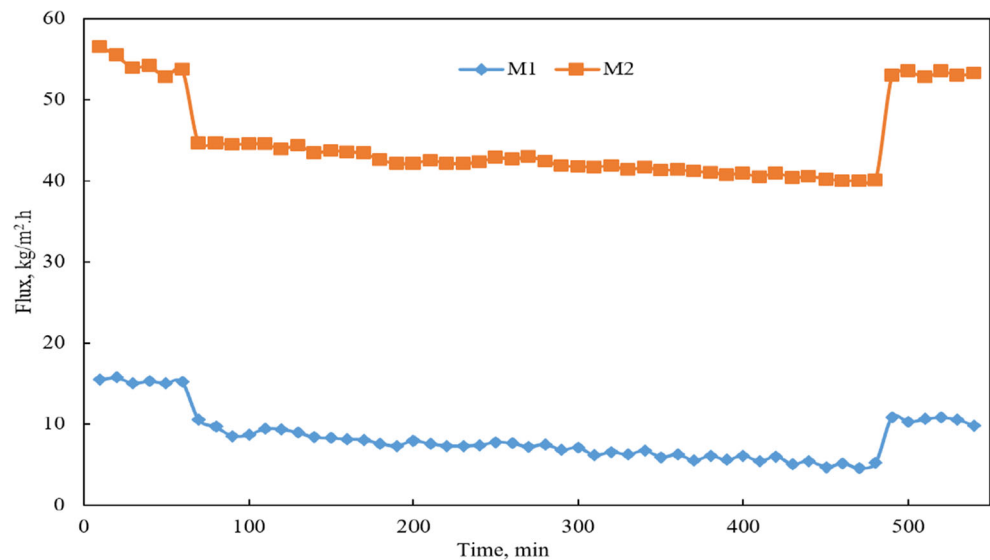


Table 6 and Fig. 13. From the results, due to the high cross-flow velocity (CFV) and hence the increase of the Reynolds number (create turbulent flow due to $Re > 4000$) so that the cross-flow setup permeation showed enhancement in comparison with dead-end setup due to polarization concentration reduction (Bagheri et al. 2019).

According to Fig. 13 and Table 5, slump less flux in membrane permeability was observed in the prolonged dye removal process. This phenomenon can be justified by a reduction in the concentration polarization behind the membrane during the examination process. The drop of the membrane flux at the M_1 (31.58% reduction) is much higher than that of the M_2 (2.33% reduction), which can be attributed to the membrane modification by the hydrophilic nanoparticle and the donation of the antifouling property for the M_2 membrane. According to the results presented, it can be obtained that the embedding of GO-CPTMS@Pd-TKHPP hydrophilic nanocomposite in the membrane matrix has improved the performance of the color removal, flux enhancement, and antifouling property (Zangeneh et al. 2019b).

Conclusion

In this work, a hydrophilic nanofiller (modified graphene oxide nanocomposite) was successfully used and blended with the bare membrane during the phase inversion to reclaim membrane flux, antifouling, and dye removal performance. The effect of modified graphene oxide in the casting solution was evaluated and chosen as the optimal membrane. The selected modified graphene oxide-PES membrane (0.1 wt.% of modified graphene oxide) exhibited better pure water flux $37.33 \text{ kg/m}^2\cdot\text{h}$ and dye rejection of 99.58 % compared to the unmodified membranes. By embedding the modified graphene oxide, membrane hydrophilicity was significantly

improved. Antifouling experiments showed that the addition of the modified graphene oxide in the casting solution led to an increment in flux recovery ratio from 58.65 to 91.76% and a decrement in irreversible fouling from 41.35 to 8.24 %. The result of long filtration in the cross-flow system revealed that the optimized membrane can be proposed for industrial wastewater treatment.

Author contribution Foad Gholami: conceptualization, data curation, formal analysis, writing – original draft

Sirus Zinadini: funding acquisition, project administration

Soheila Nakhjiri Kamrani: investigation

Ali Akbar Zinatizadeh: supervision, writing – review and editing

Kiumars Bahrami: writing – review and editing, supervision

Data availability The datasets used and/or analyzed during the current study are available from the corresponding author on reasonable request.

Declarations

Ethics approval Not applicable

Consent to participate Not applicable

Consent for publication Not applicable

Competing interests The authors declare no competing interests.

References

- Abdi G, Alizadeh A, Zinadini S, Moradi G (2018) Removal of dye and heavy metal ion using a novel synthetic polyethersulfone nanofiltration membrane modified by magnetic graphene oxide/metformin hybrid. *J Membr Sci* 552:326–335
- Ang WL, Mohammad AW, Hilal N, Leo CP (2015) A review on the applicability of integrated/hybrid membrane processes in water treatment and desalination plants. *Desalination* 363:2–18

- Asadi A, Zinatizadeh AA, Van Loosdrecht M (2016) High rate simultaneous nutrients removal in a single air lift bioreactor with continuous feed and intermittent discharge regime: process optimization and effect of feed characteristics. *Chem Eng J* 301:200–209
- Ayyaru S, Ahn Y-H (2017) Application of sulfonic acid group functionalized graphene oxide to improve hydrophilicity, permeability, and antifouling of PVDF nanocomposite ultrafiltration membranes. *J Membr Sci* 525:210–219
- Bagheri M, Akbari A, Mirbagheri SA (2019) Advanced control of membrane fouling in filtration systems using artificial intelligence and machine learning techniques: a critical review. *Process Saf Environ Prot* 123:229–252
- Bahrami K, Kamrani SN (2018) Synthesis, characterization and application of graphene palladium porphyrin as a nanocatalyst for the coupling reactions such as: Suzuki-Miyaura and Mizoroki-Heck. *Appl Organomet Chem* 32:e4102
- Balea A, Monte MC, de la Fuente E, Negro C, Blanco Á (2017) Application of cellulose nanofibers to remove water-based flexographic inks from wastewaters. *Environ Sci Pollut Res* 24:5049–5059
- Balea A, Monte MC, Fuente E, Sanchez-Salvador JL, Blanco A, Negro C (2019) Cellulose nanofibers and chitosan to remove flexographic inks from wastewaters. *Environmental Science: Water Research & Technology* 5:1558–1567
- Bouazizi A, Breida M, Achiou B, Ouammou M, Calvo JI, Aaddane A, Younssi SA (2017) Removal of dyes by a new nano-TiO₂ ultrafiltration membrane deposited on low-cost support prepared from natural Moroccan bentonite. *Appl Clay Sci* 149:127–135
- Chen J-L, Yan X-P (2010) A dehydration and stabilizer-free approach to production of stable water dispersions of graphene nanosheets. *J Mater Chem* 20:4328–4332
- Cote LJ, Kim J, Zhang Z, Sun C, Huang J (2010) Tunable assembly of graphene oxide surfactant sheets: wrinkles, overlaps and impacts on thin film properties. *Soft Matter* 6:6096–6101
- Deka JR, Liu C-L, Wang T-H, Chang W-C, Kao H-M (2014) Synthesis of highly phosphonic acid functionalized benzene-bridged periodic mesoporous organosilicas for use as efficient dye adsorbents. *J Hazard Mater* 278:539–550
- Ding S, Zhang L, Li Y, L-a H (2019) Fabrication of a novel polyvinylidene fluoride membrane via binding SiO₂ nanoparticles and a copper ferrocyanide layer onto a membrane surface for selective removal of cesium. *J Hazard Mater* 368:292–299
- Elimelech M, Phillip WA (2011) The future of seawater desalination: energy, technology, and the environment. *Science* 333:712–717
- Emam HE, Abdelhamid AE, Abdelhameed RM (2019) Refining of liquid fuel from N-containing compounds via using designed polysulfone@ metal organic framework composite film. *J Clean Prod* 218:347–356
- Fareghi-Alamdari R, Golestanzadeh M, Bagheri O (2016) meso-Tetrakis [4-(methoxycarbonyl) phenyl] porphyrinatopalladium (II) supported on graphene oxide nanosheets (Pd (II)-TMCP-Gr): synthesis and catalytic activity. *RSC Adv* 6:108755–108767
- Fathizadeh M, Xu WL, Zhou F, Yoon Y, Yu M (2017) Graphene oxide: a novel 2-dimensional material in membrane separation for water purification. *Adv Mater Interfaces* 4:1600918
- Gholami F, Zinatini S, Zinatizadeh A, Noori E, Rafiee E (2017) Preparation and characterization of an antifouling polyethersulfone nanofiltration membrane blended with graphene oxide/Ag nanoparticles. *Int J Eng Trans A Basics* 30:1425–1433
- Gholami F, Zinatizadeh A, Zinatini S, McKay T, Sibali L (2020) An innovative jet loop-airlift bioreactor for simultaneous removal of carbon and nitrogen from soft drink industrial wastewater: process performance and kinetic evaluation. *Environ Technol Innov* 19:100772
- Hairom NHH, Mohammad AW, Kadhum AAH (2014) Nanofiltration of hazardous Congo red dye: performance and flux decline analysis. *Journal of Water Process Engineering* 4:99–106
- Hegab HM, Zou L (2015) Graphene oxide-assisted membranes: fabrication and potential applications in desalination and water purification. *J Membr Sci* 484:95–106
- Hu M, Zheng S, Mi B (2016) Organic fouling of graphene oxide membranes and its implications for membrane fouling control in engineered osmosis. *Environ Sci Technol* 50:685–693
- Hua Z, Tang Z, Bai X, Zhang J, Yu L, Cheng H (2015) Aggregation and resuspension of graphene oxide in simulated natural surface aquatic environments. *Environ Pollut* 205:161–169
- Huang A, Liu Q, Wang N, Zhu Y, Jr C (2014) Bicontinuous zeolitic imidazolate framework ZIF-8@ GO membrane with enhanced hydrogen selectivity. *J Am Chem Soc* 136:14686–14689
- Huang H, Song Z, Wei N, Shi L, Mao Y, Ying Y, Sun L, Xu Z, Peng X (2013) Ultrafast viscous water flow through nanostrand-channelled graphene oxide membranes. *Nat Commun* 4:2979
- Januário EFD, Beluci NCL, Vidovix TB, Vieira MF, Bergamasco R, Vieira AMS (2020) Functionalization of membrane surface by layer-by-layer self-assembly method for dyes removal. *Process Saf Environ Prot* 134:140–148
- Koltonow AR, Huang J (2016) Two-dimensional nanofluidics. *Science* 351:1395–1396
- Lee N, Amy G, Croué J-P, Buisson H (2004) Identification and understanding of fouling in low-pressure membrane (MF/UF) filtration by natural organic matter (NOM). *Water Res* 38:4511–4523
- Lessan F, Karimi M, Arami M (2016) Tailoring the hierarchical porous structure within polyethersulfone/cellulose nanosheets mixed matrix membrane to achieve efficient dye/salt mixture fractionation. *J Polym Res* 23:171
- Li R, Ren Y, Zhao P, Wang J, Liu J, Zhang Y (2019) Graphitic carbon nitride (g-C₃N₄) nanosheets functionalized composite membrane with self-cleaning and antibacterial performance. *J Hazard Mater* 365:606–614
- Liu C, Mao H, Zheng J, Zhang S (2017a) Tight ultrafiltration membrane: preparation and characterization of the thermally resistant carboxylated cardo poly (arylene ether ketone)s (PAEK-COOH) tight ultrafiltration membrane for dye removal. *J Membr Sci* 530:1–10
- Liu G, Han K, Ye H, Zhu C, Gao Y, Liu Y, Zhou Y (2017b) Graphene oxide/triethanolamine modified titanate nanowires as photocatalytic membrane for water treatment. *Chem Eng J* 320:74–80
- Mahmodi G, Dangwal S, Zarrintaj P, Zhu M, Mao Y, McIlroy DN, Saeb MR, Vatanpour V, Ramsey JD, Kim S-J (2020a) NaA zeolite-coated meshes with tunable hydrophilicity for oil-water separation. *Sep Purif Technol* 240:116630
- Mahmodi G, Zarrintaj P, Taghizadeh A, Taghizadeh M, Manouchehri S, Dangwal S, Anil R, Ganjali MR, Ramsey JD, Kim S-J (2020b) From microporous to mesoporous mineral frameworks: an alliance between zeolite and chitosan. *Carbohydr Res* 107930:107930
- Manda BK, Worrell E, Patel MK (2014) Innovative membrane filtration system for micropollutant removal from drinking water—prospective environmental LCA and its integration in business decisions. *J Clean Prod* 72:153–166
- Modi A, Bellare J (2019) Efficient removal of dyes from water by high flux and superior antifouling polyethersulfone hollow fiber membranes modified with ZnO/cGO nanohybrid. *Journal of Water Process Engineering* 29:100783
- Moradi G, Zinatini S, Rajabi L (2020) Development of high flux nanofiltration membrane using para-amino benzoate ferroxane nanoparticle for enhanced antifouling behavior and dye removal. *Process Saf Environ Prot* 144:65–78
- Mukherjee R, Bhunia P, De S (2019) Nanofiltration range desalination by high flux graphene oxide impregnated ultrafiltration hollow fiber mixed matrix membrane. *J Clean Prod* 213:393–405

- Ng LY, Mohammad AW, Leo CP, Hilal N (2013) Polymeric membranes incorporated with metal/metal oxide nanoparticles: a comprehensive review. *Desalination* 308:15–33
- Panda SR, De S (2014) Preparation, characterization and performance of ZnCl₂ incorporated polysulfone (PSF)/polyethylene glycol (PEG) blend low pressure nanofiltration membranes. *Desalination* 347:52–65
- Papageorgiou DG, Kinloch IA, Young RJ (2015) Graphene/elastomer nanocomposites. *Carbon* 95:460–484
- Pirsaheb M, Farahani MHDA, Zinadini S, Zinatizadeh AA, Rahimi M, Vatanpour V (2019) Fabrication of high-performance antibiofouling ultrafiltration membranes with potential application in membrane bioreactors (MBRs) comprising polyethersulfone (PES) and polycitrate-alumoxane (PC-A). *Sep Purif Technol* 211:618–627
- Qian Y, Zhou C, Huang A (2018) Cross-linking modification with diamine monomers to enhance desalination performance of graphene oxide membranes. *Carbon* 136:28–37
- Sabbatini P, Yrazu F, Rossi F, Them G, Marajofsky A, de Cortalezzi MF (2010) Fabrication and characterization of iron oxide ceramic membranes for arsenic removal. *Water Res* 44:5702–5712
- Safarpour M, Vatanpour V, Khataee A (2016) Preparation and characterization of graphene oxide/TiO₂ blended PES nanofiltration membrane with improved antifouling and separation performance. *Desalination* 393:65–78
- Song Y, Sun Y, Chen M, Huang P, Li T, Zhang X, Jiang K (2020) Efficient removal and fouling-resistant of anionic dyes by nanofiltration membrane with phosphorylated chitosan modified graphene oxide nanosheets incorporated selective layer. *Journal of Water Process Engineering* 34:101086
- Vatanpour V, Madaeni SS, Moradian R, Zinadini S, Astinchap B (2011) Fabrication and characterization of novel antifouling nanofiltration membrane prepared from oxidized multiwalled carbon nanotube/polyethersulfone nanocomposite. *J Membr Sci* 375:284–294
- Wang H-W, Hu Z-A, Chang Y-Q, Chen Y-L, Zhang Z-Y, Yang Y-Y, Wu H-Y (2011) Preparation of reduced graphene oxide/cobalt oxide composites and their enhanced capacitive behaviors by homogeneous incorporation of reduced graphene oxide sheets in cobalt oxide matrix. *Mater Chem Phys* 130:672–679
- Wang Y, Zhu J, Dong G, Zhang Y, Guo N, Liu J (2015) Sulfonated halloysite nanotubes/polyethersulfone nanocomposite membrane for efficient dye purification. *Sep Purif Technol* 150:243–251
- Warsinger DM, Chakraborty S, Tow EW, Plumlee MH, Bellona C, Loutatidou S, Karimi L, Mikelonis AM, Achilli A, Ghassemi A (2018) A review of polymeric membranes and processes for potable water reuse. *Prog Polym Sci* 81:209–237
- You S-J, Semblante GU, Lu S-C, Damodar RA, Wei T-C (2012) Evaluation of the antifouling and photocatalytic properties of poly(vinylidene fluoride) plasma-grafted poly(acrylic acid) membrane with self-assembled TiO₂. *J Hazard Mater* 237:10–19
- Yuan X-T, Xu C-X, Geng H-Z, Ji Q, Wang L, He B, Jiang Y, Kong J, Li J (2020) Multifunctional PVDF/CNT/GO mixed matrix membranes for ultrafiltration and fouling detection. *J Hazard Mater* 384:120978
- Zaaba N, Foo K, Hashim U, Tan S, Liu W-W, Voon C (2017) Synthesis of graphene oxide using modified hummers method: solvent influence. *Procedia engineering* 184:469–477
- Zangeneh H, Zinatizadeh AA, Feyzi M, Zinadini S, Bahnemann DW (2018) Photomineralization of recalcitrant wastewaters by a novel magnetically recyclable boron doped-TiO₂-SiO₂ cobalt ferrite nanocomposite as a visible-driven heterogeneous photocatalyst. *Journal of environmental chemical engineering* 6:6370–6381
- Zangeneh H, Zinatizadeh AA, Zinadini S, Feyzi M, Bahnemann DW (2019a) Preparation and characterization of a novel photocatalytic self-cleaning PES nanofiltration membrane by embedding a visible-driven photocatalyst boron doped-TiO₂SiO₂/CoFe₂O₄ nanoparticles. *Sep Purif Technol* 209:764–775
- Zangeneh H, Zinatizadeh AA, Zinadini S, Feyzi M, Bahnemann DW (2019b) Preparation ultrafine L-methionine (C, N, S triple doped)-TiO₂-ZnO nanoparticles and their photocatalytic performance for fouling alleviation in PES nanocomposite membrane. *Compos Part B* 176:107158
- Zangeneh H, Zinatizadeh AA, Zinadini S, Feyzi M, Rafiee E, Bahnemann DW (2019c) A novel L-histidine (C, N) codoped-TiO₂-CdS nanocomposite for efficient visible photo-degradation of recalcitrant compounds from wastewater. *J Hazard Mater* 369:384–397
- Zhang J, Feng A, Bai J, Tan Z, Shao W, Yang Y, Hong W, Xiao Z (2017) One-pot synthesis of hierarchical flower-like Pd-Cu alloy support on graphene towards ethanol oxidation. *Nanoscale Res Lett* 12:521
- Zhang X, Li H, Wang J, Peng D, Liu J, Zhang Y (2019) In-situ grown covalent organic framework nanosheets on graphene for membrane-based dye/salt separation. *J Membr Sci* 581:321–330
- Zhou M-Y, Zhang P, Fang L-F, Zhu B-K, Wang J-L, Chen J-H, Abdallah HM (2019) A positively charged tight UF membrane and its properties for removing trace metal cations via electrostatic repulsion mechanism. *J Hazard Mater* 373:168–175
- Zhu J, Tian M, Zhang Y, Zhang H, Liu J (2015) Fabrication of a novel “loose” nanofiltration membrane by facile blending with Chitosan–Montmorillonite nanosheets for dyes purification. *Chem Eng J* 265:184–193
- Zinadini S, Zinatizadeh AA, Rahimi M, Vatanpour V, Zangeneh H (2014) Preparation of a novel antifouling mixed matrix PES membrane by embedding graphene oxide nanoplates. *J Membr Sci* 453:292–301
- Zolfogol MA, Khakyzadeh V, Moosavi-Zare AR, Rostami A, Zare A, Iranpoor N, Beyzavi MH, Luque R (2013) A highly stable and active magnetically separable Pd nanocatalyst in aqueous phase heterogeneously catalyzed couplings. *Green Chem* 15:2132–2140

Publisher's note Springer Nature remains neutral with regard to jurisdictional claims in published maps and institutional affiliations.